





# Diffusion-Weighted Imaging (DWI) With Apparent Diffusion Coefficient (ADC) Mapping as a Quantitative Imaging Biomarker for Prediction of Immunohistochemical Receptor Status, Proliferation Rate, and Molecular Subtypes of Breast Cancer

Joao V. Horvat, MD,<sup>1</sup> Blanca Bernard-Davila, MPH, MS,<sup>1</sup> Thomas H. Helbich, MD, MBA, MSc,<sup>2</sup> Michelle Zhang, MD,<sup>1</sup> Elizabeth A. Morris, MD,<sup>1</sup> Sunitha B. Thakur, MSc, PhD,<sup>3</sup>  R. Elena Ochoa-Albiztegui, MD,<sup>1</sup> Doris Leithner, MD,<sup>1</sup> Maria A. Marino, MD,<sup>1</sup>  Pascal A. Baltzer, MD,<sup>2</sup>  Paola Clauser, MD,<sup>2</sup> Panagiotis Kapetas, MD,<sup>2</sup> Zsuzsanna Bago-Horvath, MD, PhD,<sup>4</sup> and Katja Pinker, MD, PhD<sup>1,2\*</sup> 

**Background:** Diffusion-weighted imaging (DWI) with apparent diffusion coefficient (ADC) mapping is one of the most useful additional MRI parameters to improve diagnostic accuracy and is now often used in a multiparametric imaging setting for breast tumor detection and characterization.

**Purpose:** To evaluate whether different ADC metrics can also be used for prediction of receptor status, proliferation rate, and molecular subtype in invasive breast cancer.

**Study Type:** Retrospective.

**Subjects:** In all, 107 patients with invasive breast cancer met the inclusion criteria (mean age 57 years, range 32–87) and underwent multiparametric breast MRI.

**Field Strength/Sequence:** 3 T, readout-segmented echo planar imaging (rsEPI) with IR fat suppression, dynamic contrast-enhanced (DCE) T<sub>1</sub>-weighted imaging, T<sub>2</sub>-weighted turbo-spin echo (TSE) with fatsat.

**Assessment:** Two readers independently drew a region of interest on ADC maps on the whole tumor (WTu), and on its darkest part (DpTu). Minimum, mean, and maximum ADC values of both WTu and DpTu were compared for receptor status, proliferation rate, and molecular subtypes.

**Statistical Tests:** Wilcoxon rank sum, Mann–Whitney *U*-tests for associations between radiologic features and histopathology; histogram and q-q plots, Shapiro–Wilk's test to assess normality, concordance correlation coefficient for precision and accuracy; receiver operating characteristics curve analysis.

**Results:** Estrogen receptor (ER) and progesterone receptor (PR) status had significantly different ADC values for both readers. Maximum WTu ( $P = 0.0004$  and  $0.0005$ ) and mean WTu ( $P = 0.0101$  and  $0.0136$ ) were significantly lower for ER-positive tumors,

View this article online at [wileyonlinelibrary.com](http://wileyonlinelibrary.com). DOI: 10.1002/jmri.26697

Received Dec 21, 2018, Accepted for publication Feb 5, 2019.

\*Address reprint requests to: K.P., Department of Radiology, Breast Imaging Service, Memorial Sloan Kettering Cancer Center, New York NY. E-mail: [pinkerdk@mskcc.org](mailto:pinkerdk@mskcc.org)

From the <sup>1</sup>Department of Radiology, Breast Imaging Service, Memorial Sloan Kettering Cancer Center, New York, New York USA; <sup>2</sup>Department of Biomedical Imaging and Image-guided Therapy, Division of Molecular and Gender Imaging, Medical University of Vienna, Austria; <sup>3</sup>Department of Medical Physics, Memorial Sloan Kettering Cancer Center, New York, New York USA; and <sup>4</sup>Department of Pathology, Medical University of Vienna, Austria

Additional supporting information may be found in the online version of this article

This is an open access article under the terms of the Creative Commons Attribution-NonCommercial License, which permits use, distribution and reproduction in any medium, provided the original work is properly cited and is not used for commercial purposes.

while PR-positive tumors had significantly lower maximum WTu values ( $P = 0.0089$  and  $0.0047$ ). Maximum WTu ADC was the only metric that was significantly different for molecular subtypes for both readers ( $P = 0.0100$  and  $0.0132$ ) and enabled differentiation of luminal tumors from nonluminal ( $P = 0.0068$  and  $0.0069$ ) with an area under the curve of 0.685 for both readers.

**Data Conclusion:** Maximum WTu ADC values may be used to differentiate luminal from other molecular subtypes of breast cancer.

**Level of Evidence:** 3

**Technical Efficacy:** Stage 2

J. MAGN. RESON. IMAGING 2019;50:836–846.

**D**YNAMIC CONTRAST-ENHANCED magnetic resonance imaging (DCE-MRI) is the backbone of any given MRI protocol, but to address limitations in specificity and to improve breast cancer diagnosis, a plethora of functional MRI parameters, ie, diffusion-weighted imaging (DWI), proton and phosphorus MR spectroscopy, sodium imaging, blood oxygenation level-dependent imaging, and chemical exchange saturation transfer imaging are being investigated.<sup>1–7</sup> In this context, DWI with apparent diffusion coefficient (ADC) mapping is one of the most useful MRI parameter and is now often used in a multiparametric imaging setting for breast cancer detection.<sup>2,5,8,9</sup> DWI with ADC mapping provides information on tissue microstructure and cellularity that can be used for lesion characterization.

In breast cancer, the presence of estrogen receptor (ER), progesterone receptor (PR), human epidermal growth factor receptor 2 (HER2) and proliferation rate (Ki-67) are major prognostic factors guiding therapy decisions and prediction of tumor response to neoadjuvant treatment.<sup>10</sup> Immunohistochemical (IHC) tumor receptor status together with the Ki-67 proliferating index are related to tumor cellularity, vascularity, and aggressiveness. In addition, using IHC surrogates, molecular breast cancer subtypes can be defined,<sup>11</sup> which are routinely used to guide recommendations for neo- and adjuvant systemic therapies, as well as to provide valuable information on disease behavior and prognosis.<sup>12</sup> However, to date the information on receptor status and proliferation rate has to be obtained by invasive tissue sampling. Furthermore, although IHC of specimens obtained from breast biopsy and surgery are the gold standard for evaluating receptor status, it has some limitations. Disagreements in receptor status between biopsy and surgical specimen may occur in up to 20% of patients and disagreements among pathologists evaluating the same specimen are not uncommon.<sup>13–15</sup> In addition, tumor biology is subject to change over time and treatment that may lead to changes in receptor status and subtype.<sup>16</sup> Therefore, the investigation of noninvasive means to evaluate these prognostic factors is desirable.<sup>17</sup>

A major strength of DWI is that ADC is a quantitative parameter, which measurement can be used in clinical practice as a quantitative imaging biomarker (QIB).<sup>2,8,9,18</sup> DWI with ADC mapping has been proposed as a QIB for determination of tumor prognostic and predictive factors.<sup>19,20</sup> Whereas high-proliferating tumors with increased cellularity are expected to have lower ADC than low-proliferating tumors,<sup>21</sup> tumors with increased

neovascularity, greater vascular permeability, and a consecutive increase of extracellular fluid, such as HER2-positive lesions, are expected to have higher ADCs.<sup>22,23</sup> Hormone receptor-positive tumors, which are typically less aggressive, tend to have less neovascularity and therefore are expected to present with lower ADC values.<sup>21,22</sup> However, to date results on ADC as a QIB to predict receptor status are divergent. We believe that this might be due to different measurement approaches, ie, measurements of the entire tumor vs. subjectively chosen areas, which have been utilized across studies.<sup>17,18,21–29</sup> We hypothesized that ADC as a QIB can predict IHC receptor status, proliferation rate, and molecular tumor subtypes of breast cancer. Therefore, the aim of the study was to evaluate whether different ADC measurement approaches and metrics can be used for prediction of IHC tumor receptor status, proliferation rate, and molecular tumor subtype in patients with invasive breast cancer.

## Materials and Methods

### Patients

The Institutional Review Board approved this retrospective study and data analysis of a prospectively populated database (EK 510/2009). All patients gave informed written consent to be included in the database of MRI studies. The study database which consisted of 524 patients who underwent state-of-the-art MRI of the breast with T<sub>2</sub>-weighted, DCE-MRI, and DWI between December 2010 and February 2014 was queried for patients who fulfilled the following inclusion criteria: histopathologically verified invasive breast cancer with receptor status availability, 18 years or older, not pregnant, not breastfeeding, no previous treatment, and no contraindications for MRI or MRI contrast agents.

There were 264 consecutive patients who matched our search criteria. The exclusion criteria were: 1) nonmass enhancement or multiple masses; 2) pathology results demonstrating other types of cancer than invasive ductal carcinoma (IDC) or invasive lobular carcinoma (ILC); and 3) poor image quality or lesion nonvisibility on DWI. Overall, 107 patients were included in the study. The mean patient age was 57 years (range, 32–87). Patient selection is demonstrated in Fig. 1.

### MRI

All MR exams were performed with a 3 T MRI scanner (Tim Trio, Siemens, Erlangen, Germany) using a 4-channel breast coil (InVivo, Orlando, FL) with the patient positioned in the center of the magnet in the prone position. Patients underwent a standardized multiparametric MRI protocol including T<sub>2</sub>-weighted (T<sub>2w</sub> turbo spin echo)

imaging, DWI (readout-segmented echo planar imaging)<sup>1</sup> and DCE T<sub>1</sub>-weighted imaging (hybrid high spatial and temporal resolution protocol).<sup>30</sup> The MRI sequence parameters for T<sub>2</sub>-weighted and DCE-MRI are summarized in online Table S1 and for DWI in Table S2. DWI was performed before the application of contrast agent with DCE-MRI. For DCE-MRI gadoterate meglumine (Dotarem, Guerbet, France) was injected intravenously as a bolus (0.1 mmol/kg body weight) by a power injector (Spectris Solaris, Medrad, Pittsburgh, PA) at 4 mL/s, followed by a 20-mL saline flush. Contrast agent was injected 75 seconds after starting the first coronal T<sub>1</sub>-weighted volumetric interpolated breath-hold examination sequence. The total examination time was ~18:40 minutes.<sup>31</sup>

**Image Evaluation**

MRI studies were independently evaluated by two board-certified breast radiologists (J.V.H. and K.P.) with 7 and 12 years of experience, respectively, in breast MRI. The images were reviewed using the open-source DICOM viewer software OsiriX (Pixmeo SARL, Geneva, Switzerland). The breast tumors were identified on high b-value (850 s/mm<sup>2</sup>) images using DCE-MR images as anatomical guidance and their largest diameters were measured on DCE-MR images. The malignant tumors were then visually assessed on high b-value (850 s/mm<sup>2</sup>) DWI and on ADC maps.

Each radiologist chose the slice with the greatest representative portion of the tumor and manually drew: 1) a 2D region of interest (ROI) on the whole tumor (WTu) on the ADC map, and 2) a 2D ROI on the darkest part of the tumor (DpTu) on the same slice, with a minimum area of 10 mm<sup>2</sup>. The radiologists subjectively selected the DpTu region with the lowest signal intensity that could be distinguished from the remaining parts of the tumor. Figure 2 illustrates an example of ADC measurements for WTu and DpTu. Areas of necrosis, cystic degeneration, fat, and normal tissue were avoided while drawing the ROIs. The minimum, mean, and maximum ADC values of both the WTu and DpTu were recorded.

**Histopathological Results**

The histopathology results were reviewed for tumor histology, histological grade, and IHC status by one dedicated pathologist with 12 years of experience (Z.B.). Evaluation of IHC status included ER, PR, HER2, and Ki67 according to standard protocols using an automated Ventana Benchmark XT device (Ventana, Tucson, AZ). Staining results were evaluated according to current ASCO/USCAP guidelines.<sup>32,33</sup> The standard of reference was histological analysis of the surgical specimen; in patients who received neoadjuvant treatment, the biopsy results were considered the standard of reference. Tumor subtypes were classified as luminal A for either ER- or PR-positive and HER2-negative, luminal B for either ER- or PR-positive and HER2-positive, HER2-enriched for ER- and PR-negative and HER2-positive, and triple negative (TN) for ER-, PR-, and HER2-negative. A HER2 status of 0 or 1+ was considered negative, 2+ as equivocal, and 3+ as positive. Patients with equivocal HER2 were evaluated using fluorescence in situ hybridization (FISH) and considered positive if HER2 gene amplification was observed. The Ki-67 proliferation index was classified as high proliferating if staining positivity was equal to or more than 20% and low proliferating if positivity was lower than 20%.<sup>34</sup>

**Statistical Analysis**

All statistical analyses were performed with SAS 9.4 (SAS Institute, Cary, NC). Metric data values were expressed as mean, median (quartile), or percentage values, as appropriate. Associations between radiologic features (minimum, mean, and maximum WTu and DpTu ADC values) and histopathology, IHC receptor (ER, PR, HER2), and Ki-67 status were assessed using Wilcoxon rank sum and Mann-Whitney *U*-tests where appropriate. Histogram and q-q plots were examined and the Shapiro-Wilk's test was performed to assess normality. Normal distribution mean values were reported for all ADC measurements derived from Wtu and DpTu ROIs. All ADC measurements were log transformed to obtain a normal distribution when appropriate. *P*-values for log transformed features were

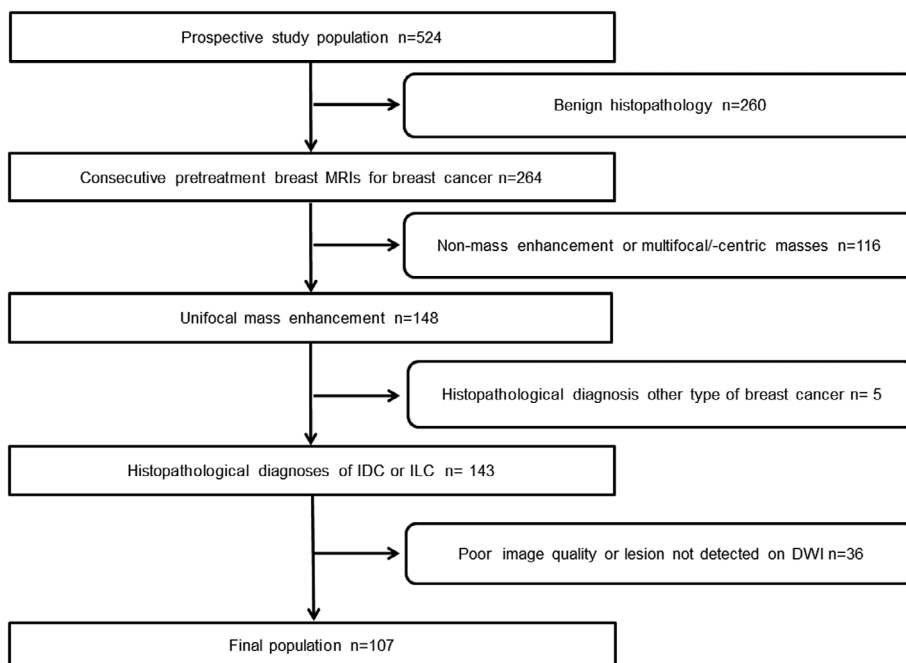


**FIGURE 1:** Flow chart of the patient selection towards final study cohort.

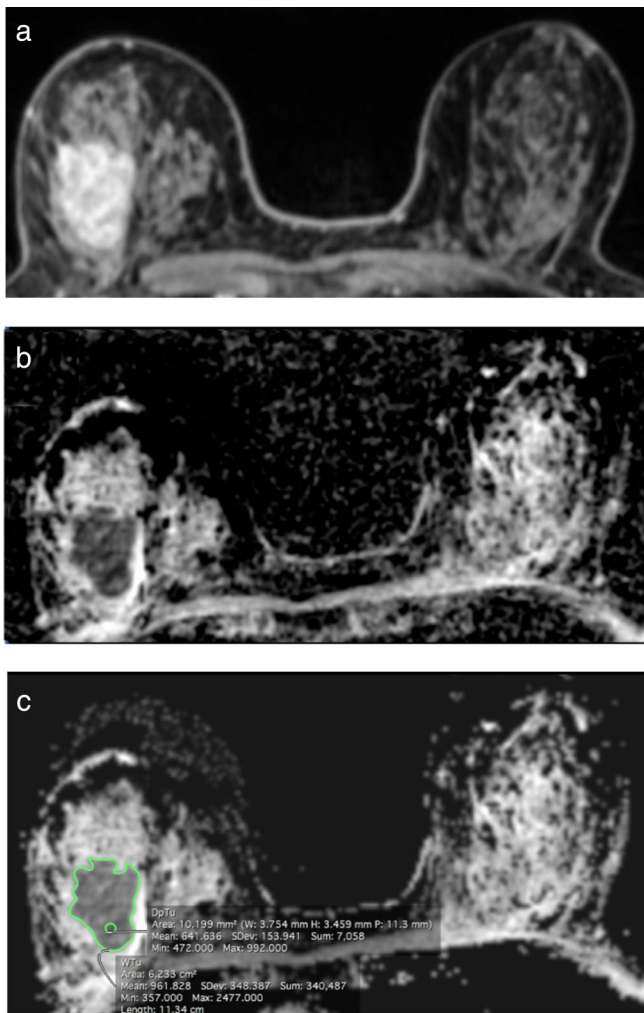


**FIGURE 2:** A 65-year-old woman with invasive ductal carcinoma of the right breast on DCE-MR images (a) and the ADC map (b). ROIs on the ADC map (c) demonstrate high maximum WTu ADC ( $2.48 \times 10^{-3}$  mm<sup>2</sup>/s) in this ER-negative, PR-negative, and HER2-positive tumor.

reported. The concordance correlation coefficient was used to measure the precision and accuracy as it relates to the agreement between two readers for each imaging parameter.<sup>35</sup> Agreement between two readings was quantified by measuring the variation from the 45° line and the line of concordance. Coefficient values closer to 1 indicate better agreement between readers. ADC measurements by the more experienced reader were used for statistical analysis. Receiver operating characteristics (ROC) curve analysis was performed. The presented sensitivities and specificities are based on this analysis. A *P*-value equal to or below 0.5 was considered to indicate a significant result.

## Results

### Histopathology

Ninety-five (89%) patients presented with IDC and 12 (11%) with ILC. ER, PR, and HER2 status was available in all 107 patients

and Ki-67 in 86. Eighty (75%) tumors were ER-positive and 27 (25%) negative. Seventy-three (68%) were PR-positive and 34 (32%) negative. Seventeen (16%) were HER2-positive and 90 (84%) were negative. Seventy (81%) patients had high proliferating and 16 (19%) had low proliferating Ki-67 status.

Based on IHC surrogates, 71 (66%) patients were classified as having luminal A, 13 (12%) luminal B, 4 (4%) HER2 enriched, and 19 (18%) TN breast cancer.

### IHC Receptor and Ki-67 Status

The mean tumor size was 33 mm (range, 13–97). The ADC values for WTu (mean, minimum, and maximum) and DpTu (mean, minimum, and maximum) stratified by IHC receptor and Ki-67 status are summarized in Table 1. ER and PR status were the only to present significantly different ADC values for both readers. Maximum WTu ADC ( $P = 0.0004$  for reader 1 and  $P = 0.0005$  for reader 2) and mean WTu ADC ( $P = 0.0101$  for reader 1 and  $P = 0.0136$  for reader 2) were significantly lower for ER-positive than for ER-negative tumors. For PR-positive tumors only maximum WTu ADC values were significantly lower than PR-negative tumors ( $P = 0.0089$  for reader 1 and  $P = 0.0047$  for reader 2). The sensitivity, specificity, and area under the curve (AUC) of both readers for the prediction of ER status using maximum WTu and mean WTu ADC and for the prediction of PR status using maximum WTu ADC are demonstrated in Table 2.

HER2-positive tumors had significantly higher maximum WTu ADC values for reader 1 ( $P = 0.0412$ ) but not for reader 2 ( $P = 0.2661$ ), and significantly higher mean WTu, minimum WTu, and minimum DpTu ADC values for reader 2 ( $P = 0.0400$ ,  $P = 0.0348$ , and  $P = 0.0447$ , respectively) but not for reader 1 ( $P = 0.0682$ ,  $P = 0.1859$ , and  $P = 0.1558$ ). Ki-67 status was only significantly different for reader 2 using the maximum DpTu ADC metric ( $P = 0.0246$ ). No other significant association was observed between the different ADC metrics and IHC status or proliferation rate. There was no statistically significant association between ADC measurements and tumor histology or grade.

### Molecular Subtypes

Maximum WTu ADC was the only metric to be significantly different for both readers among the four different molecular subtypes ( $P = 0.0100$  for reader 1 and 0.0132 for reader 2). The ADC values of the different metrics used stratified according to molecular subtypes are demonstrated in Table 3. Median maximum WTu ADC values were lower for luminal A tumors ( $2.09 \times 10^{-3}$  mm<sup>2</sup>/s for reader 1 and  $2.01 \times 10^{-3}$  mm<sup>2</sup>/s for reader 2) and higher for HER2-enriched tumors ( $2.36 \times 10^{-3}$  mm<sup>2</sup>/s for reader 1 and  $2.37 \times 10^{-3}$  mm<sup>2</sup>/s for reader 2). In addition, maximum WTu ADC enabled differentiation of luminal from nonluminal tumors ( $P = 0.0068$  for reader 1 and

**TABLE 1. Median and 25<sup>th</sup> and 75<sup>th</sup> Percentiles of ADC Measurements for WTu (Mean, Minimum, and Maximum) and DpTu (Mean, Minimum, and Maximum) Stratified by Receptor Status and Proliferation Rate**

		Ki-67																																																								
ADC Metric (x 10 <sup>-3</sup> mm <sup>2</sup> /s)		ER pos (n = 80)			ER neg (n = 27)			PR pos (n = 73)			PR neg (n = 34)			HER2 pos (n = 17)			HER2 neg (n = 90)			low (n = 16)			high (n = 70)			P																																
Max DpTu ADC (render 1)	1.03 (0.89, 1.19)	1.10 (0.93, 1.32)	1.12 (0.92, 1.40)	0.9001	1.10 (0.93, 1.36)	1.07 (0.92, 1.23)	0.4782	1.12 (0.99, 1.22)	1.10 (0.91, 1.35)	0.6763	1.22 (0.95, 1.38)	1.10 (0.96, 1.30)	0.2867	1.04 (0.90, 1.16)	1.06 (0.90, 1.20)	0.5796	1.22 (1.03, 1.37)	1.04 (0.90, 1.16)	0.0246	0.82 (0.71, 0.94)	0.81 (0.67, 0.92)	0.0806	0.95 (0.76, 1.01)	0.82 (0.72, 0.92)	0.0916	0.57 (0.40, 0.68)	0.55 (0.37, 0.69)	0.1558	0.57 (0.28, 0.85)	0.57 (0.40, 0.68)	0.4602	0.60 (0.37, 0.83)	0.61 (0.54, 0.72)	0.9072	2.05 (1.85, 2.15)	2.14 (1.96, 2.38)	0.1151	1.87 (1.73, 2.13)	2.09 (1.81, 2.33)	0.1671	1.08 (0.98, 1.19)	1.05 (0.93, 1.17)	0.6814	1.05 (0.98, 1.14)	1.02 (0.90, 1.13)	0.7018	0.11 (0.00, 0.32)	0.00 (0.00, 0.30)	0.1859	0.11 (0.00, 0.43)	0.00 (0.00, 0.40)	0.5854	0.36 (0.00, 0.54)	0.00 (0.00, 0.41)	0.0348	0.32 (0.00, 0.57)	0.06 (0.00, 0.45)	0.4401
Max DpTu ADC (render 2)	1.03 (0.89, 1.19)	1.07 (0.95, 1.26)	0.4014	1.06 (0.90, 1.22)	1.06 (0.93, 1.16)	0.9121	1.10 (0.96, 1.18)	1.06 (0.90, 1.20)	0.5796	1.22 (1.03, 1.37)	1.04 (0.90, 1.16)	0.0246	0.82 (0.71, 0.94)	0.81 (0.67, 0.92)	0.0806	0.95 (0.76, 1.01)	0.82 (0.72, 0.92)	0.0916	0.57 (0.40, 0.68)	0.55 (0.37, 0.69)	0.1558	0.57 (0.28, 0.85)	0.57 (0.40, 0.68)	0.4602	0.60 (0.37, 0.83)	0.61 (0.54, 0.72)	0.9072	2.05 (1.85, 2.15)	2.14 (1.96, 2.38)	0.1151	1.87 (1.73, 2.13)	2.09 (1.81, 2.33)	0.1671	1.08 (0.98, 1.19)	1.05 (0.93, 1.17)	0.6814	1.05 (0.98, 1.14)	1.02 (0.90, 1.13)	0.7018	0.11 (0.00, 0.32)	0.00 (0.00, 0.30)	0.1859	0.11 (0.00, 0.43)	0.00 (0.00, 0.40)	0.5854	0.36 (0.00, 0.54)	0.00 (0.00, 0.41)	0.0348	0.32 (0.00, 0.57)	0.06 (0.00, 0.45)	0.4401							
Mean DpTu ADC (render 1)	0.81 (0.70, 0.93)	0.85 (0.70, 0.97)	0.3994	0.82 (0.71, 0.94)	0.84 (0.69, 0.94)	0.9786	0.85 (0.73, 0.92)	0.81 (0.70, 0.94)	0.4610	0.91 (0.74, 1.03)	0.82 (0.71, 0.95)	0.2462	0.82 (0.68, 0.95)	0.81 (0.67, 0.92)	0.0806	0.95 (0.76, 1.01)	0.82 (0.72, 0.92)	0.0916	0.57 (0.40, 0.68)	0.55 (0.37, 0.69)	0.1558	0.57 (0.28, 0.85)	0.57 (0.40, 0.68)	0.4602	0.60 (0.37, 0.83)	0.61 (0.54, 0.72)	0.9072	2.05 (1.85, 2.15)	2.14 (1.96, 2.38)	0.1151	1.87 (1.73, 2.13)	2.09 (1.81, 2.33)	0.1671	1.08 (0.98, 1.19)	1.05 (0.93, 1.17)	0.6814	1.05 (0.98, 1.14)	1.02 (0.90, 1.13)	0.7018	0.11 (0.00, 0.32)	0.00 (0.00, 0.30)	0.1859	0.11 (0.00, 0.43)	0.00 (0.00, 0.40)	0.5854	0.36 (0.00, 0.54)	0.00 (0.00, 0.41)	0.0348	0.32 (0.00, 0.57)	0.06 (0.00, 0.45)	0.4401							
Mean DpTu ADC (render 2)	0.82 (0.68, 0.94)	0.87 (0.75, 0.93)	0.1869	0.82 (0.68, 0.95)	0.85 (0.73, 0.92)	0.5515	0.87 (0.82, 0.95)	0.81 (0.67, 0.92)	0.0806	0.95 (0.76, 1.01)	0.82 (0.72, 0.92)	0.0916	0.57 (0.40, 0.68)	0.55 (0.37, 0.69)	0.1558	0.57 (0.28, 0.85)	0.57 (0.40, 0.68)	0.4602	0.60 (0.37, 0.83)	0.61 (0.54, 0.72)	0.9072	2.05 (1.85, 2.15)	2.14 (1.96, 2.38)	0.1151	1.87 (1.73, 2.13)	2.09 (1.81, 2.33)	0.1671	1.08 (0.98, 1.19)	1.05 (0.93, 1.17)	0.6814	1.05 (0.98, 1.14)	1.02 (0.90, 1.13)	0.7018	0.11 (0.00, 0.32)	0.00 (0.00, 0.30)	0.1859	0.11 (0.00, 0.43)	0.00 (0.00, 0.40)	0.5854	0.36 (0.00, 0.54)	0.00 (0.00, 0.41)	0.0348	0.32 (0.00, 0.57)	0.06 (0.00, 0.45)	0.4401													
Min DpTu ADC (render 1)	0.54 (0.36, 0.69)	0.64 (0.50, 0.72)	0.1203	0.55 (0.00, 0.72)	0.58 (0.48, 0.69)	0.5248	0.66 (0.54, 0.72)	0.55 (0.37, 0.69)	0.1558	0.57 (0.28, 0.85)	0.57 (0.40, 0.68)	0.4602	0.60 (0.37, 0.83)	0.61 (0.54, 0.72)	0.9072	2.05 (1.85, 2.15)	2.14 (1.96, 2.38)	0.1151	1.87 (1.73, 2.13)	2.09 (1.81, 2.33)	0.1671	1.08 (0.98, 1.19)	1.05 (0.93, 1.17)	0.6814	1.05 (0.98, 1.14)	1.02 (0.90, 1.13)	0.7018	0.11 (0.00, 0.32)	0.00 (0.00, 0.30)	0.1859	0.11 (0.00, 0.43)	0.00 (0.00, 0.40)	0.5854	0.36 (0.00, 0.54)	0.00 (0.00, 0.41)	0.0348	0.32 (0.00, 0.57)	0.06 (0.00, 0.45)	0.4401	0.02 (0.00, 0.41)	0.36 (0.00, 0.54)	0.0657	0.04 (0.00, 0.43)	0.12 (0.00, 0.47)	0.3505	0.43 (0, 0.57)	0.00 (0.00, 0.41)	0.0348	0.32 (0.00, 0.57)	0.06 (0.00, 0.45)	0.4401							
Min DpTu ADC (render 2)	0.58 (0.46, 0.72)	0.68 (0.57, 0.76)	0.0587	0.58 (0.45, 0.72)	0.63 (0.53, 0.73)	0.2739	0.71 (0.58, 0.76)	0.59 (0.48, 0.72)	0.0447	0.60 (0.37, 0.83)	0.61 (0.54, 0.72)	0.9072	2.05 (1.85, 2.15)	2.14 (1.96, 2.38)	0.1151	1.87 (1.73, 2.13)	2.09 (1.81, 2.33)	0.1671	1.08 (0.98, 1.19)	1.05 (0.93, 1.17)	0.6814	1.05 (0.98, 1.14)	1.02 (0.90, 1.13)	0.7018	0.11 (0.00, 0.32)	0.00 (0.00, 0.30)	0.1859	0.11 (0.00, 0.43)	0.00 (0.00, 0.40)	0.5854	0.36 (0.00, 0.54)	0.00 (0.00, 0.41)	0.0348	0.32 (0.00, 0.57)	0.06 (0.00, 0.45)	0.4401	0.02 (0.00, 0.41)	0.36 (0.00, 0.54)	0.0657	0.04 (0.00, 0.43)	0.12 (0.00, 0.47)	0.3505	0.43 (0, 0.57)	0.00 (0.00, 0.41)	0.0348	0.32 (0.00, 0.57)	0.06 (0.00, 0.45)	0.4401										
Max WTu ADC (render 1)	2.11 (1.93, 2.32)	2.34 (2.15, 2.60)	0.0004	2.12 (1.93, 2.33)	2.26 (2.08, 2.48)	0.0089	2.33 (2.14, 2.40)	2.13 (1.93, 2.34)	0.0412	2.05 (1.85, 2.15)	2.14 (1.96, 2.38)	0.1151	1.87 (1.73, 2.13)	2.09 (1.81, 2.33)	0.1671	1.08 (0.98, 1.19)	1.05 (0.93, 1.17)	0.6814	1.05 (0.98, 1.14)	1.02 (0.90, 1.13)	0.7018	0.11 (0.00, 0.32)	0.00 (0.00, 0.30)	0.1859	0.11 (0.00, 0.43)	0.00 (0.00, 0.40)	0.5854	0.36 (0.00, 0.54)	0.00 (0.00, 0.41)	0.0348	0.32 (0.00, 0.57)	0.06 (0.00, 0.45)	0.4401	0.02 (0.00, 0.41)	0.36 (0.00, 0.54)	0.0657	0.04 (0.00, 0.43)	0.12 (0.00, 0.47)	0.3505	0.43 (0, 0.57)	0.00 (0.00, 0.41)	0.0348	0.32 (0.00, 0.57)	0.06 (0.00, 0.45)	0.4401													
Max WTu ADC (render 2)	2.03 (1.76, 2.22)	2.32 (1.98, 2.75)	0.0005	2.01 (1.75, 2.21)	2.22 (2.00, 2.40)	0.0047	2.14 (1.89, 2.35)	2.06 (1.77, 2.32)	0.2661	1.87 (1.73, 2.13)	2.09 (1.81, 2.33)	0.1671	1.08 (0.98, 1.19)	1.05 (0.93, 1.17)	0.6814	1.05 (0.98, 1.14)	1.02 (0.90, 1.13)	0.7018	0.11 (0.00, 0.32)	0.00 (0.00, 0.30)	0.1859	0.11 (0.00, 0.43)	0.00 (0.00, 0.40)	0.5854	0.36 (0.00, 0.54)	0.00 (0.00, 0.41)	0.0348	0.32 (0.00, 0.57)	0.06 (0.00, 0.45)	0.4401	0.02 (0.00, 0.41)	0.36 (0.00, 0.54)	0.0657	0.04 (0.00, 0.43)	0.12 (0.00, 0.47)	0.3505	0.43 (0, 0.57)	0.00 (0.00, 0.41)	0.0348	0.32 (0.00, 0.57)	0.06 (0.00, 0.45)	0.4401																
Mean WTu ADC (render 1)	1.03 (0.92, 1.15)	1.13 (0.97, 1.37)	0.0101	1.03 (0.92, 1.16)	1.10 (0.96, 1.23)	0.1151	1.11 (1.03, 1.19)	1.04 (0.93, 1.16)	0.0682	1.08 (0.98, 1.19)	1.05 (0.93, 1.17)	0.6814	1.05 (0.98, 1.14)	1.02 (0.90, 1.13)	0.7018	0.11 (0.00, 0.32)	0.00 (0.00, 0.30)	0.1859	0.11 (0.00, 0.43)	0.00 (0.00, 0.40)	0.5854	0.36 (0.00, 0.54)	0.00 (0.00, 0.41)	0.0348	0.32 (0.00, 0.57)	0.06 (0.00, 0.45)	0.4401	0.02 (0.00, 0.41)	0.36 (0.00, 0.54)	0.0657	0.04 (0.00, 0.43)	0.12 (0.00, 0.47)	0.3505	0.43 (0, 0.57)	0.00 (0.00, 0.41)	0.0348	0.32 (0.00, 0.57)	0.06 (0.00, 0.45)	0.4401	0.02 (0.00, 0.41)	0.36 (0.00, 0.54)	0.0657	0.04 (0.00, 0.43)	0.12 (0.00, 0.47)	0.3505	0.43 (0, 0.57)	0.00 (0.00, 0.41)	0.0348	0.32 (0.00, 0.57)	0.06 (0.00, 0.45)	0.4401							
Mean WTu ADC (render 2)	1.00 (0.90, 1.11)	1.12 (0.97, 1.23)	0.0136	1.00 (0.90, 1.11)	1.09 (0.96, 1.18)	0.7018	1.11 (1.01, 1.17)	1.01 (0.90, 1.13)	0.0400	1.05 (0.98, 1.14)	1.02 (0.90, 1.13)	0.7018	0.11 (0.00, 0.32)	0.00 (0.00, 0.30)	0.1859	0.11 (0.00, 0.43)	0.00 (0.00, 0.40)	0.5854	0.36 (0.00, 0.54)	0.00 (0.00, 0.41)	0.0348	0.32 (0.00, 0.57)	0.06 (0.00, 0.45)	0.4401	0.02 (0.00, 0.41)	0.36 (0.00, 0.54)	0.0657	0.04 (0.00, 0.43)	0.12 (0.00, 0.47)	0.3505	0.43 (0, 0.57)	0.00 (0.00, 0.41)	0.0348	0.32 (0.00, 0.57)	0.06 (0.00, 0.45)	0.4401	0.02 (0.00, 0.41)	0.36 (0.00, 0.54)	0.0657	0.04 (0.00, 0.43)	0.12 (0.00, 0.47)	0.3505	0.43 (0, 0.57)	0.00 (0.00, 0.41)	0.0348	0.32 (0.00, 0.57)	0.06 (0.00, 0.45)	0.4401										
Min WTu ADC (render 1)	0.01 (0.00, 0.32)	0.02 (0.00, 0.41)	0.4030	0.02 (0.00, 0.41)	0.01 (0.00, 0.36)	0.9858	0.26 (0, 0.51)	0.00 (0.00, 0.30)	0.1859	0.11 (0.00, 0.43)	0.00 (0.00, 0.40)	0.5854	0.36 (0.00, 0.54)	0.00 (0.00, 0.41)	0.0348	0.32 (0.00, 0.57)	0.06 (0.00, 0.45)	0.4401	0.02 (0.00, 0.41)	0.36 (0.00, 0.54)	0.0657	0.04 (0.00, 0.43)	0.12 (0.00, 0.47)	0.3505	0.43 (0, 0.57)	0.00 (0.00, 0.41)	0.0348	0.32 (0.00, 0.57)	0.06 (0.00, 0.45)	0.4401	0.02 (0.00, 0.41)	0.36 (0.00, 0.54)	0.0657	0.04 (0.00, 0.43)	0.12 (0.00, 0.47)	0.3505	0.43 (0, 0.57)	0.00 (0.00, 0.41)	0.0348	0.32 (0.00, 0.57)	0.06 (0.00, 0.45)	0.4401																
Min WTu ADC (render 2)	0.02 (0.00, 0.41)	0.36 (0.00, 0.54)	0.0657	0.04 (0.00, 0.43)	0.12 (0.00, 0.47)	0.3505	0.43 (0, 0.57)	0.00 (0.00, 0.41)	0.0348	0.32 (0.00, 0.57)	0.06 (0.00, 0.45)	0.4401	0.02 (0.00, 0.41)	0.36 (0.00, 0.54)	0.0657	0.04 (0.00, 0.43)	0.12 (0.00, 0.47)	0.3505	0.43 (0, 0.57)	0.00 (0.00, 0.41)	0.0348	0.32 (0.00, 0.57)	0.06 (0.00, 0.45)	0.4401	0.02 (0.00, 0.41)	0.36 (0.00, 0.54)	0.0657	0.04 (0.00, 0.43)	0.12 (0.00, 0.47)	0.3505	0.43 (0, 0.57)	0.00 (0.00, 0.41)	0.0348	0.32 (0.00, 0.57)	0.06 (0.00, 0.45)	0.4401	0.02 (0.00, 0.41)	0.36 (0.00, 0.54)	0.0657	0.04 (0.00, 0.43)	0.12 (0.00, 0.47)	0.3505	0.43 (0, 0.57)	0.00 (0.00, 0.41)	0.0348	0.32 (0.00, 0.57)	0.06 (0.00, 0.45)	0.4401										

ADC, Apparent Diffusion Coefficient; DpTu, Darkest Part of Tumor; ER, Estrogen Receptor; HER2, Human Epidermal Growth Factor Receptor 2; Max, Maximum; Min, Minimum; Neg, Negative; Pos, Positive; PR, Progesterone Receptor; WTu, Whole Tumor.

**TABLE 2. Sensitivity, Specificity, and Area Under the Curve of Both Readers for the Prediction of ER Status Using Maximum WTu and Mean WTu ADC and for the Prediction of PR Status Using Maximum WTu ADC**

Max WTu ADC	Sensitivity	Specificity	AUC
ER (reader 1)	90%	48%	0.730
ER (reader 2)	70%	70%	0.724
PR (reader 1)	58%	71%	0.656
PR (reader 2)	71%	68%	0.671
Mean WTu ADC	Sensitivity	Specificity	AUC
ER (reader 1)	94%	22%	0.666
ER (reader 2)	68%	63%	0.660

ADC, Apparent Diffusion Coefficient; AUC, Area Under the Curve; DpTu, Darkest Part of Tumor; ER, Estrogen Receptor; Max, Maximum; Progesterone Receptor; WTu, Whole Tumor.

$P = 0.0069$  for reader 2) with an AUC of 0.685 for both readers. ROC curves of both readers on the differentiation between luminal and nonluminal tumors are demonstrated in Fig. 3. Median values, sensitivity, specificity, and AUC for differentiation of luminal tumors from nonluminal subtypes using maximum WTu ADC for both readers are summarized in Table 4.

### Interreader Agreement

Interreader agreement of minimum, maximum, and mean ADC measurements ranged from moderate with WTu to low for DpTu and are summarized in Table 5 and illustrated in scatterplots in Fig. 4.

### Discussion

Our study demonstrated that maximum WTu ADC and to some extent mean WTu ADC can be used as a QIB for the differentiation of tumors with different receptor status in invasive breast cancer. Maximum WTu ADC was significantly different among molecular tumor subtypes for both readers and can differentiate luminal breast cancers from nonluminal subtypes. However, there is still a significant amount of overlap of ADC values among different receptor status and molecular subtypes, which reduces the accuracy of the metrics used.

There is evidence that multiparametric MRI using DCE-MRI and DWI with ADC mapping can improve the diagnostic accuracy for breast cancer.<sup>36–38</sup> Moreover, it has been proposed that ADC can be used as a noninvasive QIB to determine prognostic and predictive factors in breast cancer such as tumor grade, receptor status, proliferation rate, and

molecular subtype. However, this has often been met with limited success,<sup>2,17,19,21,23,26–29,31,39</sup> which might be due to different measurement approaches and ADC metrics used.

Park et al found that HER2-positive cancers had higher mean ADC values, but ER and PR status were not correlated with mean ADC values.<sup>23</sup> Compared with Park et al, Martinich et al and Choi et al observed lower mean ADC on ER-positive tumors, but both groups did not find any significant correlation between mean ADC and HER2.<sup>17,21</sup> Several other groups found no significant correlation between ADC and either hormone receptor or HER2 status.<sup>26,27,29</sup> In our study, mean WTu ADC values were associated with ER status for both readers, but not with PR, HER2, or Ki-67 proliferation rate. ADC mean is an average across the chosen ROI. Approaches that use an ROI that covers the entire lesion may be more effective in demonstrating the true ADC values in heterogeneous lesions. This may explain the positive results obtained with mean WTu ADC on ER status in our study.

In contrast to previous studies, we evaluated different ADC measurement approaches and metrics for their ability as a QIB to predict receptor status in invasive breast cancer. In addition to the commonly used approach of assessing round 2D ROIs placed on the area with the lowest ADC values inside the lesions, we also delineated a 2D ROI on the whole tumor and obtained minimum, mean, and maximum ADC values. In our study, maximum WTu proved to be the most useful ADC metric as a predictive and prognostic QIB. We found that maximum WTu ADC can be used to distinguish ER and PR status with greater AUCs than other metrics. Although these results are promising, larger-scale studies are necessary for confirmation before these ADC metrics can be implemented in the decision-making of patient treatment.

We also investigated interreader agreement of different ADC measurements and metrics. The moderate agreement for WTu measurement is most likely due to the fact that the size and shape of the ROIs are not identical between two readers. The low interreader agreement for DpTu is expected, as ROIs are placed after subjective radiologist's review; therefore, not necessarily the same ROI location is chosen. We show that using a WTu approach is more robust with respect to interreader agreement than using a DpTu approach, indicating that for measurements of ADC as QIB a WTu ROI approach is better suited. Previously, Lee et al performed histogram analysis from whole-tumor segmentation and demonstrated that ADC measurements derived from the entire tumor were related to ER, PR, and HER2 status.<sup>28</sup> These findings further support the results of the current study suggesting that measurements of the whole tumor area could be more accurate for the prediction of prognostic factors than subjective selected area measurements.

**TABLE 3. Median, 25<sup>th</sup>, and 75<sup>th</sup> Percentiles and P-Value of ADC Measurements for WTu (Mean, Minimum, and Maximum) and DpTu (Mean, Minimum, and Maximum) Stratified by Molecular Subtypes**

ADC Metric (x 10 <sup>-3</sup> mm <sup>2</sup> /s)	Luminal A (n = 71)	Luminal B (n = 13)	HER2-enriched (n = 4)	TN/Basal-like (n = 19)	P
Max DpTu ADC (reader 1)	1.10 (0.91, 1.35)	1.14 (1.03, 1.24)	1.06 (0.99, 1.17)	1.06 (0.87, 1.42)	0.8664
Max DpTu ADC (reader 2)	1.00 (0.88, 1.20)	1.14 (0.99, 1.24)	0.93 (0.81, 0.97)	1.09 (0.95, 1.26)	0.2954
Mean DpTu ADC (reader 1)	0.81 (0.70, 0.94)	0.85 (0.73, 0.97)	0.86 (0.73, 0.91)	0.79 (0.69, 0.97)	0.9741
Mean DpTu ADC (reader 2)	0.80 (0.67, 0.93)	0.87 (0.82, 0.97)	0.84 (0.74, 0.89)	0.87 (0.67, 0.91)	0.1852
Min DpTu ADC (reader 1)	0.53 (0.36, 0.71)	0.58 (0.54, 0.76)	0.70 (0.58, 0.70)	0.58 (0.47, 0.68)	0.4631
Min DpTu ADC (reader 2)	0.57 (0.45, 0.72)	0.71 (0.57, 0.76)	0.73 (0.65, 0.81)	0.65 (0.50, 0.73)	0.1144
Max WTu ADC (reader 1)	2.09 (1.88, 2.86)	2.33 (2.14, 2.35)	2.36 (2.20, 2.54)	2.33 (2.04, 2.54)	<b>0.0100</b>
Max WTu ADC (reader 2)	2.01 (1.70, 2.22)	2.13 (1.89, 2.33)	2.37 (2.02, 2.63)	2.28 (1.91, 2.80)	<b>0.0132</b>
Mean WTu ADC (reader 1)	1.03 (0.91, 1.14)	1.11 (1.03, 1.19)	1.10 (1.02, 1.21)	1.12 (0.96, 1.26)	0.2446
Mean WTu ADC (reader 2)	1.00 (0.89, 1.08)	1.12 (1.00, 1.17)	1.04 (0.94, 1.15)	1.12 (0.96, 1.18)	<b>0.0219</b>
Min WTu ADC (reader 1)	0.02 (0.00, 0.31)	0.08 (0.00, 0.51)	0.31 (0.13, 0.46)	0.00 (0.00, 0.19)	0.3788
Min WTu ADC (reader 2)	0.02 (0.00, 0.40)	0.43 (0.00, 0.57)	0.41 (0.25, 0.54)	0.06 (0.00, 0.55)	0.0718

ADC, Apparent Diffusion Coefficient; DpTu, Darkest Part of Tumor; HER2, Human Epidermal Growth Factor Receptor 2; Max, Maximum; Min, Minimum; TN, Triple Negative; WTu, Whole Tumor.

**TABLE 4. Median, 25<sup>th</sup>, and 75<sup>th</sup> Percentiles, P-Value, Sensitivity, Specificity, and Area Under the Curve of Maximum WTu ADC of Both Readers for the Differentiation Between Luminal and Nonluminal Breast Cancers**

ADC metric (x 10 <sup>-3</sup> mm <sup>2</sup> /s)	Luminal A/B (n = 84) median (25 <sup>th</sup> , 75 <sup>th</sup> )	Nonluminal (n = 23) median (25 <sup>th</sup> , 75 <sup>th</sup> )	P-value	Sensitivity	Specificity	AUC
Max WTu ADC (reader 1)	2.13 (1.93, 2.33)	2.33 (2.12, 2.53)	0.0068	44%	87%	0.685
Max WTu ADC (reader 2)	2.05 (1.78, 2.23)	2.28 (1.91, 2.75)	0.0069	70%	68%	0.685

ADC, Apparent Diffusion Coefficient; AUC, Area Under the Curve; Max, Maximum; WTu, Whole Tumor.

In addition to traditional prognostic and predictive factors such as age, tumor size, axillary nodes status, grade, receptor status, and the presence or absence of peritumoral vascular invasion, molecular breast cancer subtypes have been implemented in the clinical routine and are currently used to guide recommendations for neo- and adjuvant systemic therapies. In this study, we also investigated the ability of ADC as a QIB for its ability to distinguish between different molecular subtypes as well as luminal breast cancers from other subtypes. In this context, maximum WTu ADC proved to be the most useful. Maximum WTu ADC was significantly different among molecular tumor subtypes. Luminal A tumors had the lowest ADC values, while HER2-enriched lesions had the highest, which is in good agreement with previous findings from Lee et al.<sup>28</sup> In addition, maximum WTu ADC enabled a differentiation of luminal A/B vs. nonluminal subtypes. The differentiation between luminal and nonluminal tumors is of paramount clinical importance, since these are treated with endocrine therapy and may benefit less from cytotoxic chemotherapy. Improvements in DWI technology may in the future increase the accuracy of ADC metrics so it can have clinical applicability in the preoperative classification of tumor subtypes.

The pathological basis of these differences in ADC values among different receptor status and molecular subtypes relies on previous observations regarding the association of receptor status and water diffusivity.<sup>22,23</sup> Tumors that are ER-positive tend to have lower neovascularity, thus presenting lower ADC values. On the other hand, tumors that are ER-negative tend to have higher neovascularity with increased vascular permeability, thus presenting higher ADC values. Similarly, tumors that have increased cellularity are expected to have lower ADC values. Although HER2-enriched and TN tumors may present high cellularity, it is likely that neovascularity in these tumors may impact more the ADC values than cellularity, which explains the results we observed of higher maximum WTu ADC in these molecular subtypes.

Finally, we also investigated ADC as a QIB for differentiation of tumor grade and histology. In contrast to previous studies,<sup>10,20,29</sup> which reported a relation between ADC mean values and different histologies and tumor grades, we did not find any significant difference between IDC and ILC tumors or between different histological grades across all ADC metrics.

Our study has several limitations. We chose to exclude breast cancers that presented as nonmass enhancements. These have per definition interspersed areas of normal fibroglandular and fatty tissue, which, if included in the ROIs, could have falsified the measurements. We also only used 2D ROIs for the evaluation of the tumors. It has to be noted that it is possible that 3D ROIs may better reflect the ADC values within the tumors. However, manual measurement of 3D

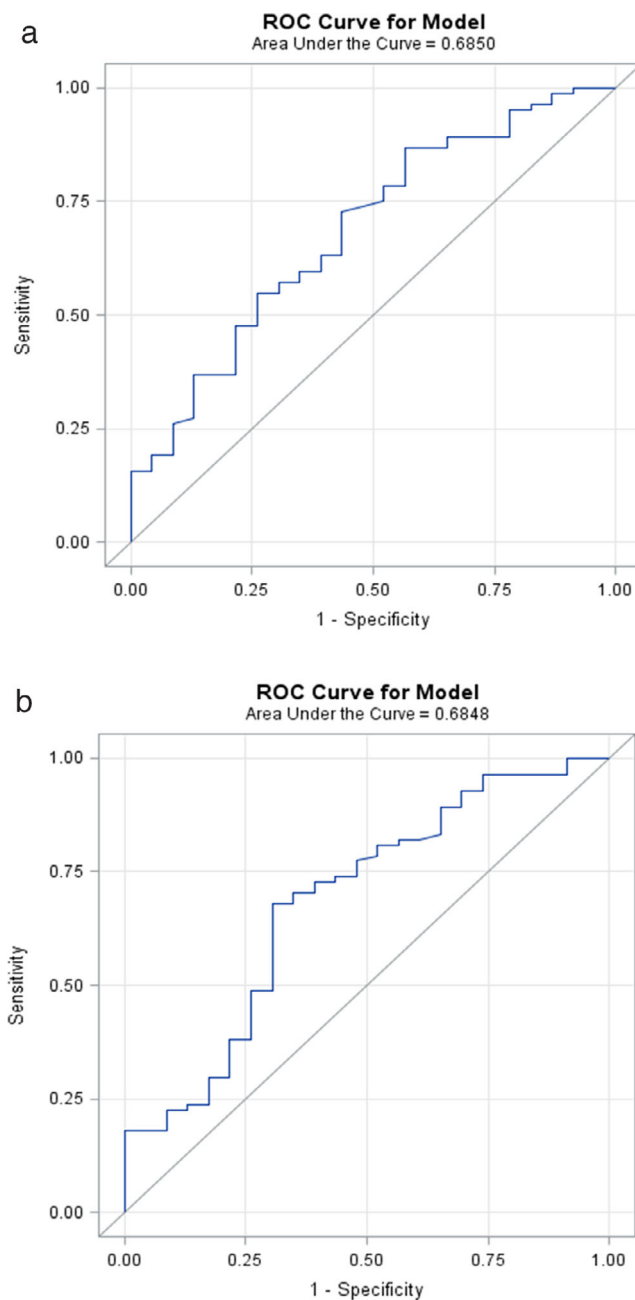


**FIGURE 3:** ROC curves of maximum WTu ADC for the differentiation between luminal and nonluminal tumors for (a) reader 1 and (b) reader 2.

ROIs is time-consuming and we aimed for an easily clinically applicable solution. It can be assumed that in the future, the development of automated tumor segmentation methods and the application of machine learning may be beneficial. Several cases where DWI was hampered by artifacts or where lesions were small ( $\leq 1$  cm) and not visible had to be excluded from analysis. However, research to improve image quality and spatial resolution of DWI is ongoing, and there have already been significant improvements with the introduction of readout-segmented echo planar imaging sequences.<sup>1</sup> Therefore, it could be expected that further advances are possible



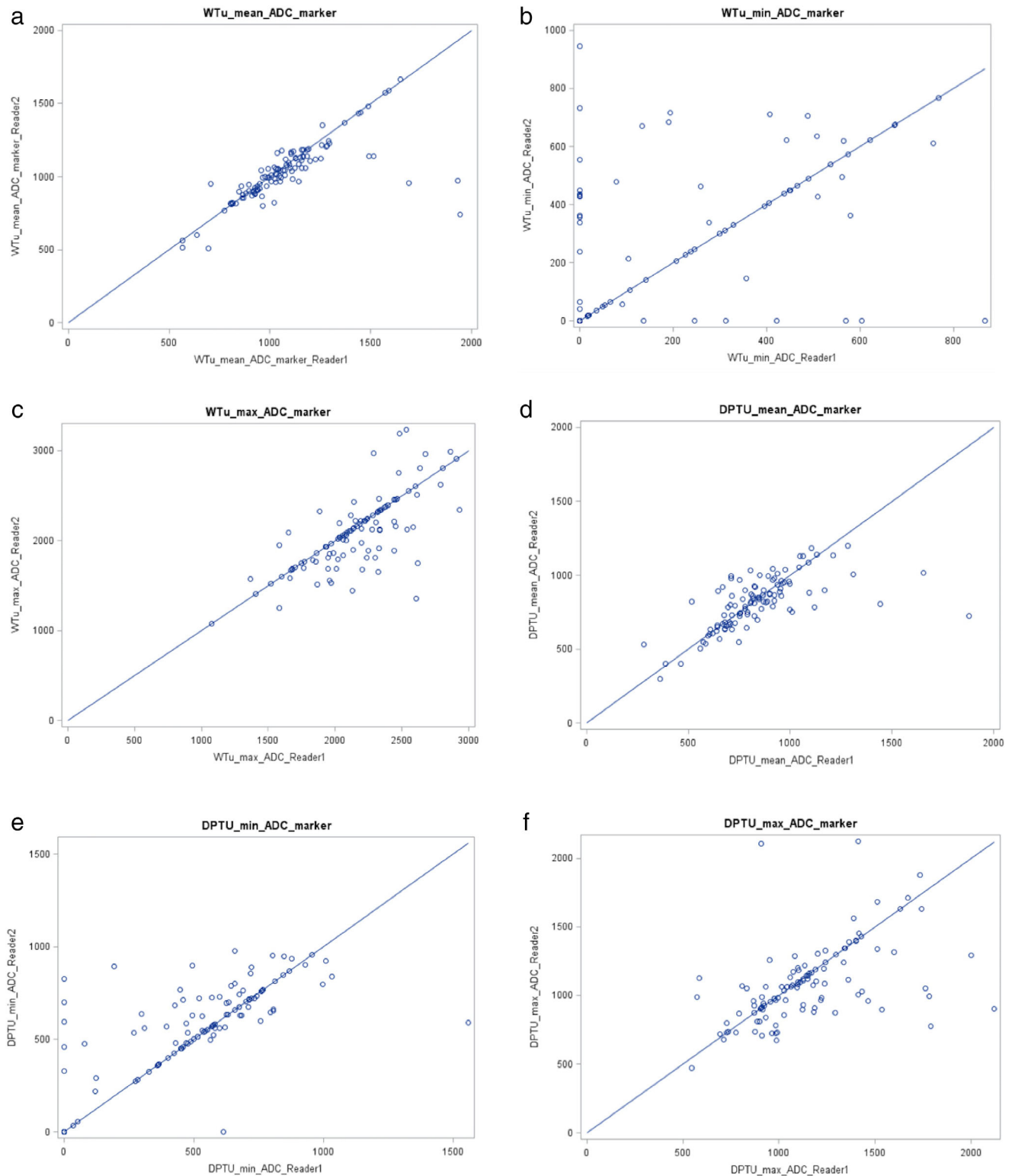


**FIGURE 4:** Scatterplots of concordance correlation coefficients between reader 1 and reader 2 regarding (a) mean WTu, (b) minimum WTu, (c) maximum WTu, (d) mean DpTu, (e) minimum DpTu, and (f) maximum DpTu.

and DWI in the future may be able to overcome its current limitations.

In conclusion, maximum WTu and mean WTu ADC values were found to be associated with hormone status of invasive breast cancers. Maximum WTu ADC can be used to

differentiate luminal cancers from other molecular subtypes of breast tumors. Other ADC measurement approaches and metrics were not significantly different for both readers regarding the determination of IHC status, molecular subtype, and Ki-67 proliferation rate.

**TABLE 5. Concordance Correlation Coefficient of Different Metrics Between the Two Readers**

ADC metric	rho-c	95 % confidence interval (CI)	Strength of agreement
Mean WTu ADC	0.712	(0.619–0.805)	Moderate
Min WTu ADC	0.561	(0.429–0.694)	Low
Max WTu ADC	0.686	(0.586–0.786)	Moderate
Mean DpTu ADC	0.609	(0.493–0.726)	Low
Min DpTu ADC	0.626	(0.512–0.740)	Low
Max DpTu ADC	0.521	(0.379–0.662)	Low

ADC, Apparent Diffusion Coefficient; DpTu, Darkest Part of Tumor; Max, Maximum; Min, Minimum; WTu, Whole Tumor.

## Acknowledgment

Contract grant sponsor: Austrian Nationalbank 'Jubiläumfond'; Contract grant number: 16219; Contract grant sponsor: 2020 – Research and Innovation Framework Programme PHC-11-2015; Contract grant number: 667211-2; Contract grant sponsor: seed grants from Siemens Austria, Novomed, and Guerbet, France; Contract grant sponsor: NIH/NCI Cancer Center; Contract grant number: P30 CA008748; Contract grant sponsor: Breast Cancer Research Foundation; Contract grant sponsor: Susan G. Komen Foundation.

The authors thank Joanne Chin for writing and editing.

## References

- Bogner W, Pinker-Domenig K, Bickel H, et al. Readout-segmented echo-planar imaging improves the diagnostic performance of diffusion-weighted MR breast examinations at 3.0 T. *Radiology* 2012;263:64–76.
- Partridge SC, DeMartini WB, Kurland BF, Eby PR, White SW, Lehman CD. Quantitative diffusion-weighted imaging as an adjunct to conventional breast MRI for improved positive predictive value. *AJR Am J Roentgenol* 2009;193:1716–1722.
- Baltzer PA, Dietzel M. Breast lesions: Diagnosis by using proton MR spectroscopy at 1.5 and 3.0 T—Systematic review and meta-analysis. *Radiology* 2013;267:735–746.
- Schmitt B, Trattnig S, Schlemmer HP. CEST-imaging: A new contrast in MR-mammography by means of chemical exchange saturation transfer. *Eur J Radiol* 2012;81(Suppl 1):S144–146.
- Pinker K, Helbich TH, Morris EA. The potential of multiparametric MRI of the breast. *Br J Radiol* 2017;90:20160715.
- Wallace TE, Patterson AJ, Abeyakoon O, et al. Detecting gas-induced vasomotor changes via blood oxygenation level-dependent contrast in healthy breast parenchyma and breast carcinoma. *J Magn Reson Imaging* 2016;44:335–345.
- Zaric O, Pinker K, Zbyn S, et al. Quantitative sodium MR imaging at 7 T: Initial results and comparison with diffusion-weighted imaging in patients with breast tumors. *Radiology* 2016;280:39–48.
- Tan SL, Rahmat K, Rozalli FI, et al. Differentiation between benign and malignant breast lesions using quantitative diffusion-weighted sequence on 3 T MRI. *Clin Radiol* 2014;69:63–71.
- Cheaney S, Rahbar H, Dontchos BN, Javid SH, Rendi MH, Partridge SC. Apparent diffusion coefficient values may help predict which MRI-detected high-risk breast lesions will upgrade at surgical excision. *J Magn Reson Imaging* 2017;46:1028–1036.
- Cipolla V, Santucci D, Guerrieri D, Drudi FM, Meggiorini ML, de Felice C. Correlation between 3T apparent diffusion coefficient values and grading of invasive breast carcinoma. *Eur J Radiol* 2014;83:2144–2150.
- Ahn HJ, Jung SJ, Kim TH, Oh MK, Yoon HK. Differences in clinical outcomes between luminal A and B type breast cancers according to the St. Gallen Consensus 2013. *J Breast Cancer* 2015;18:149–159.
- Baba S, Isoda T, Maruoka Y, et al. Diagnostic and prognostic value of pretreatment SUV in 18F-FDG/PET in breast cancer: Comparison with apparent diffusion coefficient from diffusion-weighted MR imaging. *J Nucl Med* 2014;55:736–742.
- Mann GB, Fahey VD, Feleppa F, Buchanan MR. Reliance on hormone receptor assays of surgical specimens may compromise outcome in patients with breast cancer. *J Clin Oncol* 2005;23:5148–5154.
- Burge CN, Chang HR, Apple SK. Do the histologic features and results of breast cancer biomarker studies differ between core biopsy and surgical excision specimens? *Breast* 2006;15:167–172.
- Orlando L, Viale G, Bria E, et al. Discordance in pathology report after central pathology review: Implications for breast cancer adjuvant treatment. *Breast* 2016;30:151–155.
- Pisco AO, Huang S. Non-genetic cancer cell plasticity and therapy-induced stemness in tumour relapse: 'What does not kill me strengthens me'. *Br J Cancer* 2015;112:1725–1732.
- Martincich L, Deantoni V, Bertotto I, et al. Correlations between diffusion-weighted imaging and breast cancer biomarkers. *Eur Radiol* 2012;22:1519–1528.
- Bickel H, Pinker K, Polanec S, et al. Diffusion-weighted imaging of breast lesions: Region-of-interest placement and different ADC parameters influence apparent diffusion coefficient values. *Eur Radiol* 2017;27:1883–1892.
- Durando M, Gennaro L, Cho GY, et al. Quantitative apparent diffusion coefficient measurement obtained by 3.0Tesla MRI as a potential non-invasive marker of tumor aggressiveness in breast cancer. *Eur J Radiol* 2016;85:1651–1658.
- Costantini M, Belli P, Rinaldi P, et al. Diffusion-weighted imaging in breast cancer: Relationship between apparent diffusion coefficient and tumour aggressiveness. *Clin Radiol* 2010;65:1005–1012.
- Choi SY, Chang YW, Park HJ, Kim HJ, Hong SS, Seo DY. Correlation of the apparent diffusion coefficient values on diffusion-weighted imaging with prognostic factors for breast cancer. *Br J Radiol* 2012;85:e474–479.
- Karan B, Pourbagher A, Torun N. Diffusion-weighted imaging and (18) F-fluorodeoxyglucose positron emission tomography/computed tomography in breast cancer: Correlation of the apparent diffusion

- coefficient and maximum standardized uptake values with prognostic factors. *J Magn Reson Imaging* 2016;43:1434–1444.
23. Park SH, Choi HY, Hahn SY. Correlations between apparent diffusion coefficient values of invasive ductal carcinoma and pathologic factors on diffusion-weighted MRI at 3.0 Tesla. *J Magn Reson Imaging* 2015; 41:175–182.
  24. Guvenc I, Akay S, Ince S, et al. Apparent diffusion coefficient value in invasive ductal carcinoma at 3.0 Tesla: Is it correlated with prognostic factors? *Br J Radiol* 2016;89:20150614.
  25. Jeh SK, Kim SH, Kim HS, et al. Correlation of the apparent diffusion coefficient value and dynamic magnetic resonance imaging findings with prognostic factors in invasive ductal carcinoma. *J Magn Reson Imaging* 2011;33:102–109.
  26. Kim SH, Cha ES, Kim HS, et al. Diffusion-weighted imaging of breast cancer: Correlation of the apparent diffusion coefficient value with prognostic factors. *J Magn Reson Imaging* 2009;30:615–620.
  27. Kitajima K, Yamano T, Fukushima K, et al. Correlation of the SUVmax of FDG-PET and ADC values of diffusion-weighted MR imaging with pathologic prognostic factors in breast carcinoma. *Eur J Radiol* 2016; 85:943–949.
  28. Lee HS, Kim SH, Kang BJ, Baek JE, Song BJ. Perfusion parameters in dynamic contrast-enhanced MRI and apparent diffusion coefficient value in diffusion-weighted MRI: Association with prognostic factors in breast cancer. *Acad Radiol* 2016;23:446–456.
  29. Nakajo M, Kajiya Y, Kaneko T, et al. FDG PET/CT and diffusion-weighted imaging for breast cancer: Prognostic value of maximum standardized uptake values and apparent diffusion coefficient values of the primary lesion. *Eur J Nucl Med Mol Imaging* 2010;37:2011–2020.
  30. Pinker K, Moy L, Sutton EJ, et al. Diffusion-weighted imaging with apparent diffusion coefficient mapping for breast cancer detection as a stand-alone parameter: Comparison with dynamic contrast-enhanced and multiparametric magnetic resonance imaging. *Invest Radiol* 2018 [Epub ahead of print].
  31. Pinker K, Bickel H, Helbich TH, et al. Combined contrast-enhanced magnetic resonance and diffusion-weighted imaging reading adapted to the "Breast Imaging Reporting and Data System" for multiparametric 3-T imaging of breast lesions. *Eur Radiol* 2013;23:1791–1802.
  32. Hammond ME, Hayes DF, Wolff AC, Mangu PB, Temin S. American Society of Clinical Oncology/College of American Pathologists guideline recommendations for immunohistochemical testing of estrogen and progesterone receptors in breast cancer. *J Oncol Pract* 2010;6: 195–197.
  33. Wolff AC, Hammond MEH, Allison KH, et al. Human Epidermal growth factor receptor 2 testing in breast cancer: American Society of Clinical Oncology/College of American Pathologists Clinical Practice Guideline focused update. *J Clin Oncol* 2018;36:2105–2122.
  34. Dowsett M, Nielsen TO, A'Hern R, et al. Assessment of Ki67 in breast cancer: Recommendations from the International Ki67 in Breast Cancer working group. *J Natl Cancer Inst* 2011;103:1656–1664.
  35. Lin LI. A concordance correlation coefficient to evaluate reproducibility. *Biometrics* 1989;45:255–268.
  36. Partridge SC, DeMartini WB, Kurland BF, Eby PR, White SW, Lehman CD. Quantitative diffusion-weighted imaging as an adjunct to conventional breast MRI for improved positive predictive value. *AJR Am J Roentgenol* 2009;193:1716–1722.
  37. Ei Khoulil RH, Jacobs MA, Mezban SD, et al. Diffusion-weighted imaging improves the diagnostic accuracy of conventional 3.0-T breast MR imaging. *Radiology* 2010;256:64–73.
  38. Baltzer A, Dietzel M, Kaiser CG, Baltzer PA. Combined reading of contrast enhanced and diffusion weighted magnetic resonance imaging by using a simple sum score. *Eur Radiol* 2016;26:884–891.
  39. Iaconi C, Thakur SB, Dershaw DD, Brooks J, Fry CW, Morris EA. Impact of fibroglandular tissue and background parenchymal enhancement on diffusion weighted imaging of breast lesions. *Eur J Radiol* 2014;83:2137–2143.